Oxidative Stress Promotes Peroxiredoxin Hyperoxidation and Attenuates Pro-survival Signaling in Aging Chondrocytes*

John A. Collins[‡], Scott T. Wood[‡], Kimberly J. Nelson[§], Meredith A. Rowe[‡¶], Cathy S. Carlson[∥], Susan Chubinskaya[**], **Leslie B. Poole[§], Cristina M. Furdui[¶], and Richard F. Loeser[‡1]**

From the [‡]Division of Rheumatology, Allergy and Immunology and the Thurston Arthritis Research Center, University of North Carolina at Chapel Hill, Chapel Hill, North Carolina 27599, the Departments of [§]Biochemistry and [¶]Internal Medicine, Section on Molecular Medicine, Wake Forest School of Medicine, Winston-Salem, North Carolina 27157, the [∥]Department of Veterinary Population Medicine, University of Minnesota College of Veterinary Medicine, St. Paul, Minnesota 55108, and the [**]Department of Pediatrics, Rush University Medical Center, Chicago, Illinois 60612

Oxidative stress-mediated post-translational modifications of redox-sensitive proteins are postulated as a key mechanism underlying age-related cellular dysfunction and disease progression. Peroxiredoxins (PRX) are critical intracellular antioxidants that also regulate redox signaling events. Age-related osteoarthritis is a common form of arthritis that has been associated with mitochondrial dysfunction and oxidative stress. The objective of this study was to determine the effect of aging and oxidative stress on chondrocyte intracellular signaling, with a specific focus on oxidation of cytosolic PRX2 and mitochondrial PRX3. Menadione was used as a model to induce cellular oxidative stress. Compared with chondrocytes isolated from young adult humans, chondrocytes from older adults exhibited higher levels of PRX1–3 hyperoxidation basally and under conditions of oxidative stress. Peroxiredoxin hyperoxidation was associated with inhibition of pro-survival Akt signaling and stimulation of pro-death p38 signaling. These changes were prevented in cultured human chondrocytes by adenoviral expression of catalase targeted to the mitochondria (MCAT) and in cartilage explants from MCAT transgenic mice. Peroxiredoxin hyperoxidation was observed *in situ* in human cartilage sections from older adults and in osteoarthritic cartilage. MCAT transgenic mice exhibited less age-related osteoarthritis. These findings demonstrate that age-related oxidative stress can disrupt normal physiological signaling and contribute to osteoarthritis and suggest peroxiredoxin hyperoxidation as a potential mechanism.

Aging is characterized by an inability to maintain homeostasis resulting in a progressive loss of function and is associated with many chronic conditions including cancer, type II diabetes, neurodegenerative disease, cardiovascular disease, and osteoarthritis (1, 2). Although several theories aimed at explaining the aging phenotype have been suggested, an age-related imbalance between the production of reactive oxygen species (ROS)[2] and the antioxidant capacity of the cell has been identified as a contributing factor (3–5). Although the original free radical theory of aging focused on accumulation of cellular damage from excessive ROS as a cause for aging and age-related conditions, more recent studies suggest that disturbances in redox signaling that result from age-related oxidative stress are likely to play a key role (5–7). Increased levels of ROS caused by mitochondrial dysfunction, one of the hallmarks of aging, have been proposed to contribute to age-related oxidative stress, but the underlying mechanisms for how this increase causes a disruption in cell signaling leading to cell and tissue dysfunction is poorly understood (1, 4, 8).

Recent advances in redox signaling recognize that reversible post-translational oxidative modifications of reactive protein cysteine thiols mediated by controlled production of H_2O_2 regulate key signal transduction events (9, 10). The cysteine-dependent peroxiredoxins (PRXs), which display high reactivity toward H_2O_2, have recently been postulated to act not only as important intracellular antioxidants but also as direct participants in redox signaling events through the relay of oxidizing equivalents to target proteins containing reactive thiols (11–13). During the PRX catalytic cycle, H_2O_2 oxidizes the sulfhydryl group of the peroxidatic cysteine of PRX to form sulfenic acid (PRX-SOH), which can condense with the resolving cysteine of an adjacent PRX subunit to form an intersubunit disulfide bond. Alternatively, PRX-SOH can condense with a thiol on a nearby target protein thus transferring the oxidizing equivalent, as has been shown for the redox-sensitive protein Orp1 (14). Oxidoreductases including thioredoxin serve as an additional level of regulation because of their capacity to reduce the oxidized PRX or the PRX target protein (13).

Under high levels of H_2O_2, hyperoxidation of PRX to the sulfinylated (PRX-SO_2H) and sulfonylated (PRX-SO_3H) forms can occur, leading to enzymatic inactivation and inhibition of peroxidase function (11, 15). Given that PRXs are major intracellular antioxidants, inactivation by hyperoxidation would

[1] To whom correspondence should be addressed: Thurston Arthritis Research Center, 3300 Thurston Bldg., CB#7280, University of North Carolina at Chapel Hill, Chapel Hill, NC 27599-7280. Tel.: 919-966-7042; E-mail: Richard_loeser@med.unc.edu.

[2] The abbreviations used are: ROS, reactive oxygen species; PRX, peroxiredoxin; MCAT, mitochondrial catalase; OA, osteoarthritis; IGF-1, insulin-like growth factor 1; IAM, iodoacetamide; NEM, *n*-ethylmaleimide; BAD, BCL-associated agonist of cell death; ANOVA, analysis of variance.

allow H_2O_2 to accumulate and react with cysteines in proteins that are normally slower to react than PRXs, providing an alternative to the relay mechanism for redox regulation of signaling (11). Hyperoxidized PRXs, at least in the PRX-SO_2H form, can be reduced by ATP-dependent sulfiredoxin; however, this reaction occurs at a much slower rate than thioredoxin reduction of PRX disulfides (16). If H_2O_2 and other ROS rise to levels that overwhelm the antioxidant capacity of the cell, then oxidative stress occurs, which is associated with a disruption in normal physiologic signaling (9, 13, 17). Whether PRX hyperoxidation and the subsequent disruption in signaling may underlie the altered redox signaling seen in aging has not been fully explored, and little to no data exist to support this mechanism in primary human cells.

We investigated PRX hyperoxidation as a potential mechanism for disrupted cell signaling in aging by examining its role in osteoarthritis (OA). OA represents the most common form of joint disease and is a primary cause of chronic disability in older adults. Pain and loss of function in OA are the result of a slow, progressive destruction of joint tissues including articular cartilage (18, 19). Cartilage destruction is thought to be the consequence of an imbalance between matrix synthesis and matrix degradation, which is mediated by chondrocytes, the resident cells in cartilage. OA directly correlates with increasing age and with an age-related increase in ROS levels, possibly because of a reduction in antioxidant capacity, as well as mitochondrial dysfunction (20–24).

We chose to focus on the redox regulation of the chondrocyte insulin-like growth factor-1 (IGF-1) signaling pathway because of previous studies demonstrating that IGF-1 promotes cartilage matrix synthesis and chondrocyte survival while reducing chondrocyte catabolic activity (25, 26). Disrupted pro-anabolic IGF-1 signaling has been implicated in the pathogenesis of OA, and age-associated reductions in the chondrocyte response to IGF-1 have been associated with oxidative stress (26, 27). The aim of this study was to examine whether menadione-induced oxidative stress could promote chondrocyte PRX hyperoxidation in an age-related manner and determine whether this was associated with disrupted IGF-1 signaling, chondrocyte cell death, and osteoarthritis.

Experimental Procedures

Antibodies and Reagents—Antibodies purchased from Cell Signaling Technology were to phospho-Akt (Ser[473] and Thr[308]), total Akt, phospho-p38 (Thr[180]/Tyr[182]), total p38, phospho-ERK (Thr[202]/Tyr[204]), total ERK, phospho-IGF receptor (Tyr[1135]), total IGF receptor, phospho-JNK (Thr[183]/Tyr[185]), total JNK, phospho-MKK3 (Ser[189])/MKK6 (Ser[207]), total MKK3/6, phospho-BAD (Ser[136]), total BAD, total PRAS40 (a proline-rich Akt substrate), and total COX IV, thioredoxin 1, and thioredoxin reductase 2. Antibodies to PRXSO$_{2/3}$, PRX1, PRX2, PRX3, and catalase were from Abcam. Antibodies to phospho-PRAS40 (Thr[246]) were from Upstate Cell Signaling Solutions. The antibody to sulfiredoxin was a kind gift from Dr. Sue-Goo Rhee. The Premo™ roGFP-based cellular hydrogen peroxide sensor (Orp1-roGFP) was purchased from Molecular Probes, Life Technologies. SB203580 p38 inhibitor was purchased

from CalBiochem. Menadione, *N*-ethylmaleimide (NEM), catalase, and iodoacetamide (IAM) were purchased from Sigma-Aldrich.

Human Primary Chondrocyte Isolation and Culture—Normal human cartilage was obtained from the ankle joints (talus) of tissue donors provided by the Gift of Hope Organ and Tissue Donor Network (Itasca, IL) through an agreement with Rush University Medical Center (Chicago, IL). The tissue was inspected for any gross evidence of damage, and only normal appearing tissue was used. The ages of tissue donors ranged from 27 to 75 years. Chondrocytes were isolated and cultured as described (25).

Animals—Generation of transgenic mice overexpressing human catalase targeted to the mitochondria (MCAT) has been previously described (28). All MCAT founder mice were a kind gift from Dr. Peter Rabinovitch (University of Washington, Seattle, WA) and were provided on the C57BL/6NCRl background and subsequently crossed onto the C57Bl/6NJ background. Control mice were wild-type littermates of MCAT transgenic mice. For all cell signaling studies using cartilage explants, 4-week-old female MCAT mice and their age-matched littermate wild-type controls were used. A total of 72 mice were used for these investigations (36 MCAT and 36 wild type).

Mouse Femoral Head Cartilage Explant Isolation and Culture—All mice were euthanized by CO_2 asphyxiation followed by cervical dislocation. Femoral head cartilage explants from the hip joints of 4-week-old mice were isolated by removal of the capital femoral epiphysis from the underlying bone with forceps. Femoral head cartilage explants were cultured in DMEM/Ham's F12 medium plus 10% FBS for 48 h to allow for recovery after removal from the joint. Explants were changed to serum-free conditions overnight prior to experimental treatments. To prepare chondrocyte lysates, femoral head cartilage explants were suspended in 300 μl of standard lysis buffer (containing 20 mM Tris-HCl, 150 mM NaCl, 1 mM Na$_2$EDTA, 1 mM EGTA, 1% Triton, 2.5 mM sodium pyrophosphate, 1 mM β-glycerophosphate, 1 mM Na$_3$VO$_4$, 1 μg/ml leupeptin (Cell Signaling Technology) with PMSF (Sigma), and phosphatase inhibitor mixture 2 (Sigma) in ceramic bead tubes (MOBIO Laboratories; 1.4-mm beads). The samples were homogenized in a Precellys homogenization device (Bertin Technologies) for three 40-s cycles at 6,500 rpm. After homogenization, samples were centrifuged for 5 min at 13,000 rpm to pellet tissue debris, and lysates were transferred to a clean 1.5-ml microcentrifuge tube for analysis.

Adenoviral Transduction—An adenoviral construct encoding catalase targeted to the mitochondria (MCAT) was purchased from the Gene Transfer Vector Core of the University of Iowa. Chondrocytes were transduced with the MCAT adenovirus upon reaching 70% confluency. The MCAT adenovirus (4×10^8 viral particles/ml) was added to serum-free medium containing 1 M CaCl$_2$ (25 μl/ml media), and chondrocytes were incubated for 2 h at 37 °C. Chondrocytes were washed twice with serum-free medium and cultured in 10% media for 48 h. Overnight incubation in serum-free medium preceded experimental treatments. A null vector control was used to test for nonspecific effects of viral transduction.

Analysis of Mitochondrial Catalase Expression—Mitochondrial fractions from human monolayer chondrocytes were isolated using a mitochondrial isolation kit for tissue (Thermo Scientific). Total protein in the mitochondrial fraction was measured by BCA assay, and catalase expression was analyzed by immunoblot.

Quantification of ROS Production—Menadione has been shown to induce mitochondrial and cellular oxidative stress through redox cycling (29, 30) and was therefore used as a model to induce oxidative stress in the present study. Cellular H_2O_2 levels were quantified using the Premo™ cellular hydrogen peroxide sensor (Life Technologies) Orp1-roGFP as per the manufacturer's instructions. Plasmid DNA encoding Orp1-roGFP was delivered into the cell via baculovirus transduction. Human primary chondrocytes were plated in monolayer in black-walled, cover glass-bottomed Petri dishes (SPL Lifesciences Co., Ltd.), allowing for visualization of live cells with a confocal microscope. Cover glass surfaces were functionalized in an air-fed plasma cleaner (Harrick Plasma) for 10 min, immediately coated with fibronectin for 1 h at 37 °C, and washed with PBS prior to cell seeding. Chondrocytes were transduced with Orp1-roGFP redox sensor immediately after plating at an multiplicity of infection of 80 pfu for 48 h in a 37 °C humidified 5% CO_2 incubator. Cells were serum-starved overnight prior to experimental incubations.

The Orp1-roGFP was excited at 405 nm using a diode laser and at 488 nm using an argon laser. Signal was collected at 513 nm for both image channels. Samples were imaged with a period of 10 s. Four single-cell image sets were acquired per sample at 1,890× using a GaAsP detector on a Zeiss LSM 880 with a voxel size of 800 nm × 800 nm × 0.85 μm, a pixel dwell time of 1.4 μs, and no averaging. Images were collected for 1 min prior to stimulation to establish baseline H_2O_2 levels; then menadione (25 μM) was added, and samples were imaged every 10 s for a further 2 min.

Images were analyzed in ImageJ v1.49m (31) with the FIJI plugin set based on the sensitized FRET method (32). Briefly, images were segmented and subsequently masked by adding the 405- and 488-nm images at each time point and applying a threshold using the default ImageJ thresholding algorithm. H_2O_2 levels were then determined on a pixel by pixel basis using the following equation at each time point,

$$I = \frac{405 \; ex}{488 \; ex}$$ (Eq. 1)

where I corresponds to H_2O_2 levels, and 405 *ex* and 488 *ex* correspond to the intensity of each respective image channel. Individual cells were excluded from statistical analysis if the cell appeared to exhibit any blebbing, necrosis, or cell detachment throughout the course of the experiment.

Analysis of PRX Oxidation—Confluent human chondrocyte monolayers were cultured in serum-free DMEM/Ham's F12 medium overnight prior to treatment. For experiments analyzing PRX oxidation, 25 μM menadione was used to induce oxidative stress. Human chondrocyte monolayers were washed twice with 1× Dulbecco's phosphate-buffered saline and lysed for 30 min in standard lysis buffer with PMSF and phosphatase

inhibitor mixture 2 at 4 °C. To measure PRX oxidation, including hyperoxidation, we supplemented the lysis buffer with the alkylating agent IAM at 20 mM to alkylate reduced thiols at the time of lysis and included catalase at 200 units/ml to remove H_2O_2 from the lysis buffer. At lysis, PRXs reacting stoichiometrically with residual H_2O_2 rapidly form covalent dimers detectable as higher molecular weight bands on a nonreducing immunoblot. Hyperoxidized PRXs, however, are unable to dimerize and are observed as monomers under nonreducing conditions (33).

We also used a method outlined by Cox *et al.* (33) that incorporates treating the cultured cells with NEM just prior to lysis to facilitate the observation of the reduced, oxidized, and hyperoxidized forms of PRXs. The NEM pretreatment alkylates thiols before the lysis buffer is added, which more efficiently blocks the oxidation of PRXs that may occur during cell lysis. NEM is used rather than IAM because NEM freely enters cells and alkylates intracellular thiols more efficiently at the pH of the cell culture medium. For this method, human chondrocytes were treated with menadione for the indicated times, washed in Dulbecco's phosphate-buffered saline, and pretreated with an NEM alkylating buffer (40 mM HEPES, 50 mM NaCl, 1 mM EGTA, 200 units/ml catalase, 100 mM NEM, PMSF, and phosphatase inhibitor mixture 2, pH 7.4) for 10 min prior to lysis. NEM alkylating buffer was then removed and replaced with lysis buffer containing 200 units/ml catalase and 100 mM NEM, PMSF, and phosphatase inhibitor mixture 2 (pH 7.4). Cell lysates were centrifuged at 13,000 rpm for 10 min to remove the insoluble fraction, and lysates were then subjected to reducing and nonreducing immunoblots as appropriate.

For lysis of mouse femoral cap explants, cap explants were collected, cultured, and lysed as described above. For mouse femoral caps that received NEM prior to lysis, femoral caps were incubated in 300 μl of 100 mM NEM alkylating buffer for 10 min prior to addition of 300 μl of lysis buffer containing NEM (100 mM), catalase (200 units/ml), PMSF, and phosphatase inhibitor mixture 2 (pH 7.4).

Protein contents of human and mouse lysates were quantified using the Pierce Micro BCA kit (Thermo Scientific). Approximately 15 μg (human chondrocytes) or 20 μg (mouse femoral cap cartilage) of protein/sample was combined with 5× nonreducing lane marker (Thermo Scientific) in the presence or absence of 10% β-mercaptoethanol (for reducing and nonreducing conditions respectively). Lysates were boiled and immunoblotted as previously described (34). Immunoblots for total PRX2 or PRX3 under nonreducing conditions were used as loading controls. Densitometric analysis was performed using ImageJ software.

Analysis of Chondrocyte Intracellular Signaling—For analysis of cell signaling, chondrocytes were incubated in serum-free conditions overnight prior to treatment with 25 μM menadione or 50 ng/ml IGF-1 for the indicated time points. For menadione pretreatment experiments, cells were treated with 25 μM menadione for 30 min prior to treatment with 50 ng/ml IGF-1 for the indicated times. Immunoblotting and analysis was performed as described above under reducing conditions. Analysis of phosphoproteins was conducted using phosphospecific antibodies, and blots were stripped and reprobed with antibodies to

the total protein as a loading control. For p38 inhibition studies, cells were pretreated for 30 min with 10 μM SB203580 prior to menadione treatment. Cell survival in response to menadione treatment was monitored using the LIVE/DEAD® cell assay kit (Molecular Probes) as described previously (34).

Immunohistochemistry—Cartilage sections were a kind gift from Dr. Martin Lotz (Scripps Research Institute, La Jolla, CA). Human cartilage surfaces were graded macroscopically using a modified Outerbridge scoring system and the International Cartilage Repair Society knee map as previously reported (35). For these experiments, younger donors were <50 years old, and older donors were ≥50 years old. The age cut-off for young and old donors was chosen based on a previous study from our group that demonstrated a decline in the response to IGF-1 and altered signaling under conditions of oxidative stress in chondrocytes from donors older than 50 years (27). The average age of younger cartilage was 41.3 ± 6.1 years (range, 36–48) with a Total Knee Macroscopic Cartilage Score of 57.75 ± 2.8 corresponding to Grade I (minimal changes). Normal older cartilage had an average age of 73.3 ± 4.3 years (range, 68–76) with a Total Knee Macroscopic Cartilage Score of 65.75 ± 7.1 corresponding to grade III (mild changes). Osteoarthritic cartilage had an average age of 79.3 ± 13.6 years (range, 64–90) and a Total Knee Macroscopic Cartilage Score of 127.5 ± 28.8 corresponding to Grade IV (severe changes). Immunohistochemistry protocols were performed as previously described (36). Sections blocked with DAKO protein were incubated with anti-PRX-SO$_{2/3}$ antibody (Abcam, 1:1000 dilution in DAKO antibody diluent) overnight at 4 °C. DAKO Envision™ + System HRP-labeled polymer was used to recognize the primary antibody according to the manufacturer's instructions. Images were taken with an Olympus BX60 microscope and analyzed with ImageJ software.

Mouse Knee Joint Histology—Mouse knee joints were available from six MCAT and five wild-type mice that were 18–33 months of age at necropsy (kind gift from Drs. Piper Treuting and Peter Rabinovitch, University of Washington School of Medicine). One joint from each mouse was processed, sectioned, stained, and scored for lesions as previously described (37) using the Articular Cartilage Structure scoring scheme. The Articular Cartilage Structure score is based on a scale of 0–12, where 0 is a smooth and completely intact articular cartilage surface, and 12 represents fibrillation and/or clefts and/or loss of cartilage involving the full thickness of articular cartilage involving more than two-thirds of the plateau or condyle. Scores from the medial and lateral tibial plateaus were obtained and combined to generate a sum Articular Cartilage Structure score. A single observer blinded to mouse genotype performed the scoring.

Statistical Analysis—The data were analyzed using GraphPad Prism version 6 (GraphPad Software, Inc.). Statistical analysis was performed on all data sets, and significant differences were determined by *t* test or a one-way or two-way ANOVA with a Dunnett's or Tukey HSD post hoc correction as appropriate. The results are presented as mean values ± S.E. from a minimum of three independent biological replicates. The exact number of independent samples for each experiments is pro-

vided in the figure legends. A level of $p = <0.05$ was considered to be significant.

Study Approval—Use of human tissue was in accordance with the Institutional Review Board at the Rush University Medical Center and the University of North Carolina at Chapel Hill. All animal studies were approved by the University of North Carolina Animal Care and Use Committee

Results

Menadione Increases Intracellular ROS in Human Chondrocytes—To model oxidative stress and determine the effects on signaling, we treated primary human chondrocytes with menadione, which has been shown to induce production of excessive levels of cellular ROS through redox cycling (29, 30). Because chemical probes commonly used to detect intracellular ROS lack specificity for the type of ROS produced, we used a recently developed H_2O_2 sensor, Orp1-roGFP (38), to determine whether menadione induced H_2O_2 in cultured human chondrocytes. The addition of menadione to human chondrocytes expressing Orp1-roGFP led to a significant increase in Orp1-roGFP oxidation within 20 s, an effect that was maintained over the 4-min time course studied, indicating that menadione increases cellular H_2O_2 levels in a rapid and sustained manner (Fig. 1).

Human Chondrocytes Isolated from Older Adults Are More Susceptible to PRX Hyperoxidation—The ability of ROS to promote hyperoxidation of PRXs was assessed by treating cells with menadione and using an anti-PRXSO$_{2/3}$ antibody that specifically detects the hyperoxidized sulfinic (SO$_2$) and sulfonic (SO$_3$) forms of PRX1–4. Using antibodies to specific PRXs, we were able to identify PRX1, 2, and 3 in the same region as the bands recognized by the PRXSO$_{2/3}$ antibody (Fig. 2A). Chondrocytes from older donors (average age 63 ± 12 years) exhibited increased basal levels of hyperoxidized PRX in unstimulated conditions when compared with younger donors (38 ± 10 years), and the time-dependent increase in PRX hyperoxidation in response to menadione treatment was greater in older chondrocytes when compared with younger chondrocytes (Fig. 2, B–D). These findings are consistent with age-associated oxidative stress in chondrocytes, resulting in increased susceptibility to an oxidative challenge.

Because oxidation of PRX leads to formation of an intersubunit disulfide bond between adjacent PRX subunits, disulfide-linked PRX dimers (either with two disulfides, or with one disulfide and one monomer in hyperoxidized state) can be visualized on immunoblots from nonreducing gels, whereas the fully hyperoxidized PRX is unable to dimerize and therefore remains primarily in the monomeric form. In response to menadione treatment, cytosolic PRX2 was observed at two molecular masses (Fig. 2E). The oxidized form with at least one disulfide was present at ~44 kDa, and the monomeric, fully hyperoxidized form was present at ~22 kDa. A time-dependent increase in hyperoxidized PRX2 was observed (Fig. 2, E–G), corroborating our observations using anti-PRXSO$_{2/3}$. Chondrocytes isolated from older donors exhibited greater PRX2 hyperoxidation than cells from younger donors (Fig. 2G).

Similarly, menadione-induced ROS led to significant hyperoxidation of mitochondrial PRX3, particularly in the cells from
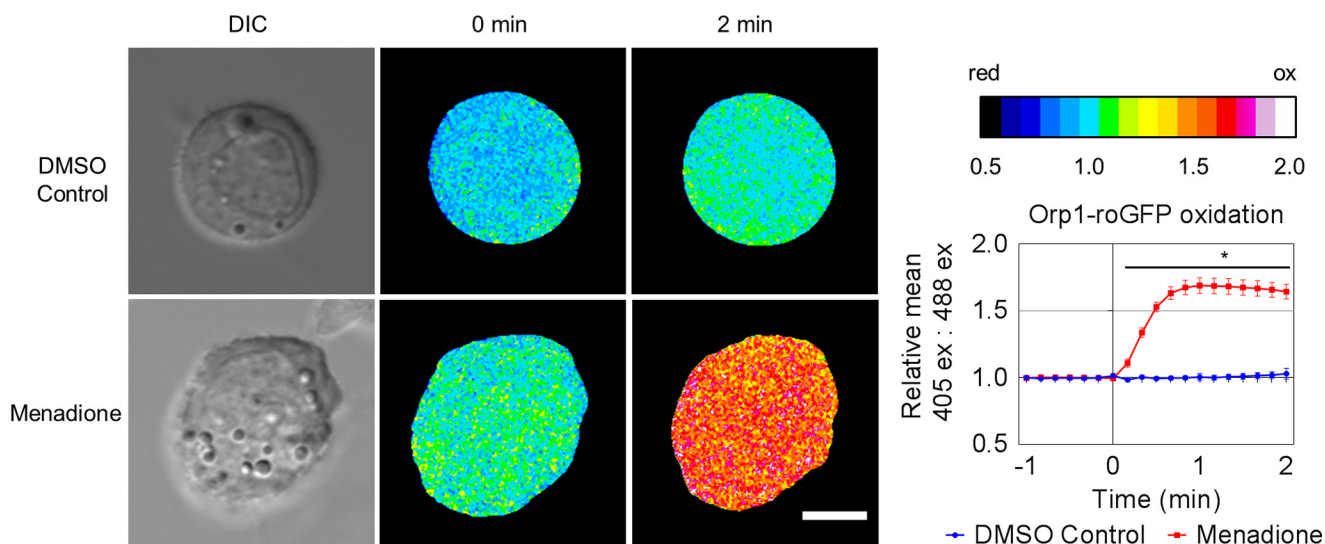
FIGURE 1. Generation of intracellular H_2O_2 in human articular chondrocytes treated with menadione. Human articular chondrocytes were transduced with a baculovirus that expresses the H_2O_2 redox sensor Orp1-roGFP. The cells were treated with or without 25 μM menadione, and the images were collected and analyzed as detailed in the methods. Images from one representative cell for control and menadione-treated conditions are shown in heat map format. *Scale bar*, 5 μM. Quantified data from 10 individual cells were taken from three independent donors. The data are presented as means ± S.E. showing the relative mean 405:488 ratio. *Asterisks* represent significant differences comparing menadione-treated chondrocytes to DMSO control. *, $p < 0.05$ (*t* test). *DIC*, differential interference contrast.

older donors (Fig. 2, *H–J*). However, in contrast to the findings for PRX2, PRX3 presented with a major dimeric band at ~38 kDa along with lower MW bands between 31 and 38 kDa, which likely represent mixed-disulfides containing at least one oxidized PRX3 peroxidatic cysteine (Fig. 2*H*). We also cannot exclude the possibility of hyperoxidized PRX3 in the bands between 31 and 38 kDa. As expected, under reducing conditions PRX2 and PRX3 ran as major monomeric bands at 22 and 24 kDa, respectively, consistent with the size of the fully reduced forms, which did not change with age (Fig. 2, *E* and *H*). The finding that chondrocytes from older adults were more susceptible to both PRX2 and PRX3 hyperoxidation induced by menadione further supports an age-related loss of reducing capacity related to basal levels of oxidative stress and not to reductions in the protein levels of PRX2 or PRX3.

Because chondrocytes are routinely serum-starved prior to experimental treatments to analyze cell signaling events, we examined the effects of serum and serum-free conditions on basal PRX oxidation. No significant differences in oxidation or hyperoxidation of PRXs were observed in the presence or absence of serum (Fig. 3, *A* and *B*).

To further examine the redox state of chondrocyte PRXs, we used NEM to alkylate reduced thiols after menadione treatment but just prior to cell lysis to block free thiol groups and prevent further oxidation or unwanted thiol-disulfide exchange that might occur early in cell lysis (33). Comparative analysis of PRX oxidation in response to menadione using either IAM added to the cell lysis buffer or NEM treatment prior to lysis are presented in Fig. 3 (*C–E*). Detection of hyperoxidized PRXs using the $PRXSO_{2/3}$ antibody was similar (Fig. 3*C*), indicating that the hyperoxidation observed in response to menadione was not due to artifactual oxidation during cell lysis. However, when we analyzed PRX2 and PRX3 oxidation on nonreducing gels, treatment with NEM prior to lysis allowed for improved

identification of the reduced monomeric, oxidized dimeric, and hyperoxidized monomeric forms of PRX.

We next examined whether the PRX oxidation induced by menadione could be altered by transducing chondrocytes with an adenoviral vector that expresses catalase targeted to the mitochondria (MCAT). Evaluation of mitochondrial and cytosolic fractions revealed that the MCAT construct was highly expressed in the mitochondria with small amounts of catalase also detected in the cytosol (Fig. 4*A*). Using NEM pretreatment to alkylate thiols prior to lysis, expression of MCAT was noted to block the menadione-induced PRX hyperoxidation (Fig. 4, *B* and *C*). Analysis of PRX2 and PRX3 on nonreducing gels showed the presence of the reduced monomeric form of PRX2 and PRX3 in samples from cells that were not treated with menadione and in cells where oxidation was inhibited by MCAT expression (Fig. 4, *D* and *E*). Menadione treatment oxidized PRX2 and PRX3 within 5 min in chondrocytes expressing null virus, evidenced by the complete disappearance of the reduced monomer and an increase in the oxidized dimeric form of the protein. Oxidized dimers were maintained until 30 min but declined at 60 min when an increase in hyperoxidized monomeric PRX was observed. The identification of the monomeric band that appeared at the later time points as the hyperoxidized PRX (rather than reduced PRX which runs at the same position) is consistent with the bands seen on $PRXSO_{2/3}$ immunoblots at this time point and with previous studies that used this technique to examine PRX hyperoxidation on nonreducing gels (33). Although menadione treatment still led to oxidized dimers of PRX2 and 3 in MCAT expressing chondrocytes, hyperoxidized PRXs in the monomeric form were not detected (Fig. 4, *B*, *D*, and *E*).

Hyperoxidized PRX Is Observed in Human Cartilage from Older Adults and in Osteoarthritic Cartilage—Having found that PRX hyperoxidation could be observed in cultured chon-
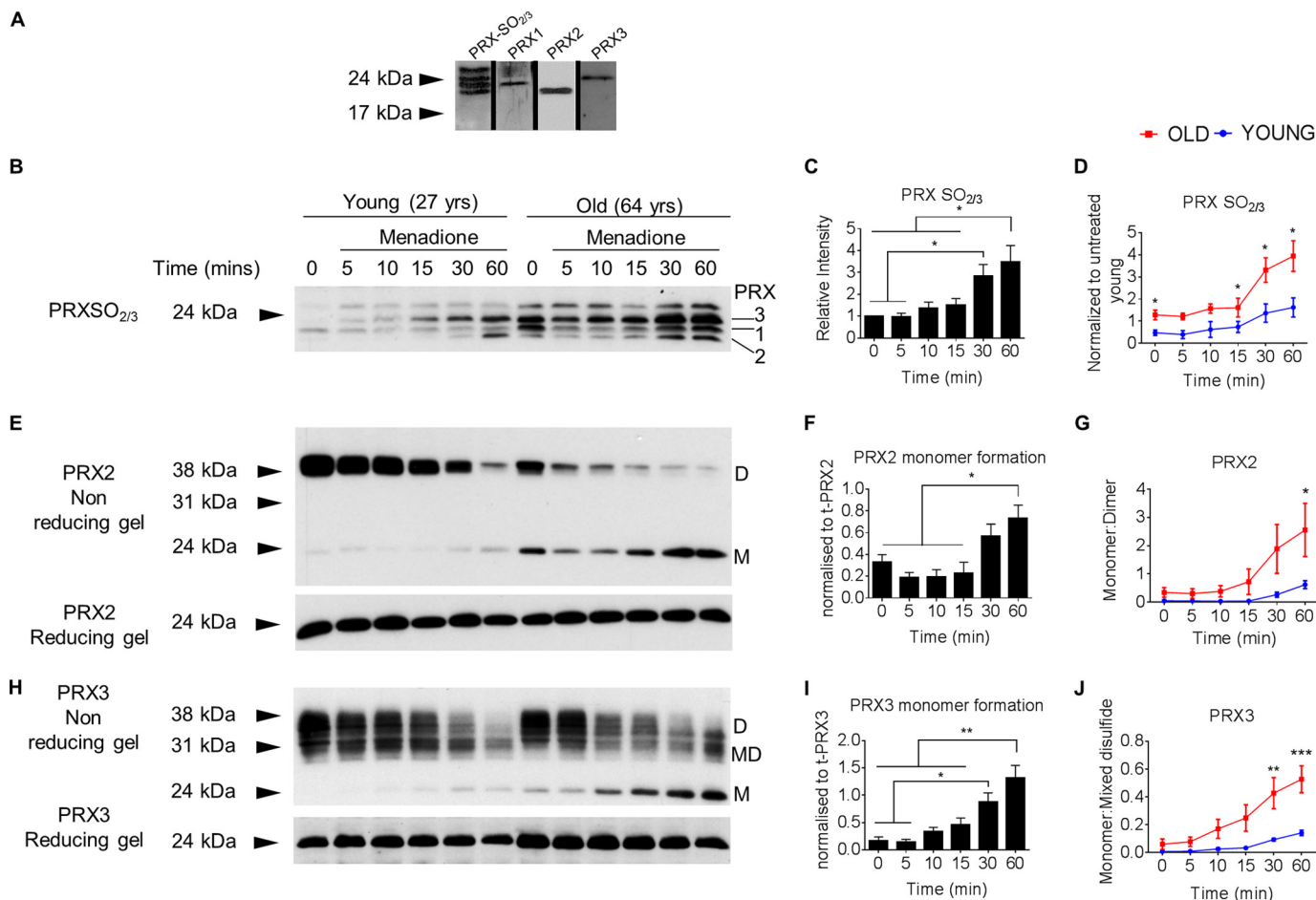
FIGURE 2. **Effect of menadione-induced oxidative stress and age on PRX oxidation in human articular chondrocytes.** Confluent human articular chondrocytes cultured in serum-free medium were treated for the indicated times with 25 μM menadione to induce oxidative stress. After treatments, cell lysates were prepared in lysis buffer containing 20 mM iodoacetamide to alkylate reduced thiols at lysis. *A*, human chondrocytes were treated with menadione for 60 min. The sample was loaded onto four lanes of a 12% gel. Each lane was separated by molecular weight marker, and the gel was run under reducing conditions. After protein transfer to membranes, individual lanes were cut out and probed with antibodies to $PRXSO_{2/3}$, PRX1, PRX2, or PRX3 to confirm the band location of each protein. Comparative analysis confirmed the locations of PRX1–3. *B*, hyperoxidized PRXs from older and younger chondrocytes were detected using an antibody that reacts with PRX 1–4 when it is in the $PRX-SO_{2/3}$ state. Specific PRXs are labeled. *C*, densitometric analysis from immunoblots of $n = 6$ donors, independent of age. The data are normalized to time 0 untreated controls. *D*, quantification of $PRXSO_{2/3}$, normalized to untreated controls from young donors, comparing chondrocytes from older ($n = 3$; average age, 63 ± 12 years; range, 50–75 years) and younger ($n = 3$; average age, 38 ± 10 years; range, 27–48 years) donors. *E*, immunoblots probed for PRX2 under nonreducing conditions (*top panel*) showing oxidized dimers (labeled *D* on blots) and hyperoxidized monomers (labeled *M* on blots). Immunoblotting for PRX2 under reducing conditions was used as a loading control (*lower panel*). *F*, densitometric analysis of PRX2 hyperoxidized monomer from $n = 6$ independent donors, independent of age. *G*, quantification of the PRX2 monomer:dimer ratio from the same donors as in *D*. *H*, immunoblots probed for PRX3 under nonreducing conditions (*top panel*). Hyperoxidized monomer is labeled *M* on blots, mixed dimers are labeled *MD* on blots, and oxidized dimer is labeled *D* on blots. Immunoblotting for PRX3 under reducing conditions was used as a loading control (*lower panel*). *I*, densitometric analysis of PRX3 hyperoxidized monomer from $n = 6$ independent donors, independent of age. *J*, quantification of the PRX3 monomer:mixed disulfide ratio from same donors as in *D*. The data are presented as means $\pm$ S.E. *Asterisks* represent significant differences between younger and older chondrocytes. *, $p < 0.05$; **, $p < 0.01$; ***, $p < 0.0001$ (ANOVA). *yrs*, years.

drocytes, we determined whether PRX hyperoxidation is present in cartilage *in vivo*. For this, we evaluated the levels of $PRXSO_{2/3}$ in normal human knee joint cartilage sections obtained from young adults (41 ± 6 years) and older adults (73 ± 5 years) and from older adult (79 ± 14 years) OA joints. Low numbers of cells staining for $PRXSO_{2/3}$ were seen in young normal cartilage with the few positive cells restricted to the superficial zones (Fig. 5). Older and OA cartilage had significantly greater numbers of $PRXSO_{2/3}$ positive cells that were present throughout the depth of the articular cartilage. A significant increase in $PRXSO_{2/3}$ positively stained cells in OA cartilage compared with older cartilage was also observed (Fig. 5), consistent with elevated levels of ROS in aging and a further increase in OA cartilage.

Oxidative Stress Inhibits Akt Signaling and Promotes p38 Signaling in Chondrocytes—IGF-1 treatment of normal human chondrocytes under basal conditions stimulated phosphorylation of the IGF-1 receptor and the downstream kinase Akt within 5 min, and phosphorylation was maintained over the 90-min time course (Fig. 6, *A–C*). IGF-1 treatment did not stimulate p38 phosphorylation, whereas ERK phosphorylation was strong and sustained (Fig. 6, *A*, *D*, and *E*). In contrast, menadione treatment to induce oxidative stress did not stimulate phosphorylation of the IGF-1 receptor or Akt at any time point, whereas it increased phosphorylation of p38 and ERK (Fig. 6).

Pretreatment with menadione to induce oxidative stress prior to addition of IGF-1 had no effect on IGF-1 receptor phosphorylation but inhibited IGF-1-stimulated phosphorylation of
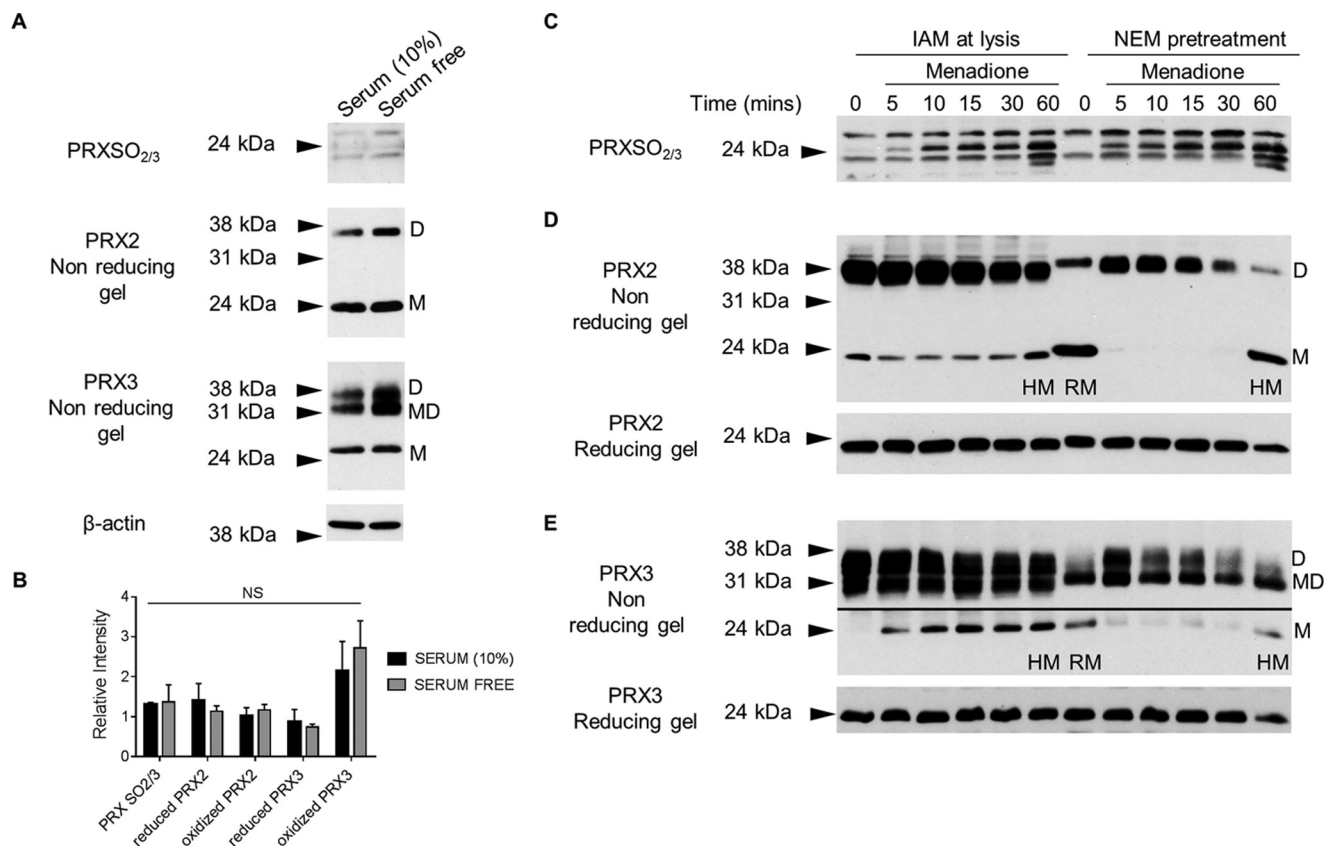
FIGURE 3. **The effects of serum-free culture and cell lysis conditions on PRX oxidation.** *A*, confluent human chondrocytes were either cultured in the presence of serum (10%) or serum-starved for 16 h, and basal levels of reduced, oxidized, and hyperoxidized PRX2 and PRX3 were detected by immunoblot. Monomeric PRX is labeled *M* on blots, and dimeric bands are labeled *D* on blots. PRX3 mixed disulfides are labeled MD on blots. *B*, densitometric analysis from immunoblots of $n = 3$ donors, independent of age. The data are normalized to β-actin loading control. The data are presented as means $\pm$ S.E. *NS* denotes nonsignificant differences between treatments. *C*, PRX hyperoxidation in human chondrocytes treated with IAM at lysis or NEM pretreatment (10 min) prior to NEM at lysis was detected with the antibody to PRX-SO$_{2/3}$. *D* and *E*, under nonreducing conditions, immunoblots for total PRX2 and PRX3 allowed for direct comparison of the IAM and NEM pretreatment methods to detect the redox status of PRXs. Monomeric bands are labeled *M* on blots, reduced monomers are labeled *RM* on blots, and hyperoxidized monomers are labeled *HM* on blots. PRX3 presented with an oxidized dimer (labeled *D* on blots), as well as a lower mixed disulfide band (labeled *MD* on blots). *Solid lines* on blots are used to separate different exposures from the same immunoblot.

Akt (Fig. 6, *A–C*). Phosphorylation of proline-rich Akt substrate (PRAS40), a direct substrate of Akt (39), was analyzed as a marker of Akt kinase activity and was significantly increased with IGF-1 treatment and inhibited by menadione pretreatment (Fig. 6F). Addition of IGF-1 to cells pretreated with menadione did not alter p38 or ERK phosphorylation when compared with menadione alone. Phosphorylation of JNK was not observed under any treatment tested (data not shown). These data demonstrate that under conditions resulting in chondrocyte PRX hyperoxidation, IGF-1-mediated Akt phosphorylation is attenuated, whereas p38 phosphorylation is increased consistent with the concept of oxidative stress disrupting normal physiologic signaling.

Expression of Mitochondrially Targeted Catalase Promotes Akt Phosphorylation and Attenuates Phosphorylation of Pro-apoptotic Signaling Proteins under Conditions of Oxidative Stress—We next assessed the ability of MCAT expression to modulate phosphorylation events in chondrocytes under oxidative stress. Expression of MCAT using adenoviral transduction led to a significant increase in basal phosphorylation of AKT at both Ser[473] and Thr[308] when compared with null empty vector control and no virus conditions (Fig. 7, *A–C*). Importantly, MCAT expression blocked the ability of menadione to inhibit Akt

phosphorylation. Phosphorylation of Akt represents a key pro-survival pathway in chondrocytes, in part because of direct phosphorylation and inhibition of the pro-apoptotic protein BAD at Ser[136] (40, 41). MCAT expression significantly increased BAD Ser[136] phosphorylation compared with null vector and no virus conditions, and the values mirrored the trend observed for Akt phosphorylation (Fig. 7, *A* and *D*).

Phosphorylation of ERK increased in a time-dependent manner in response to menadione treatment, but differences between MCAT expression, null empty vector, and no virus controls were not observed (Fig. 7, *A* and *E*). In contrast, MCAT expression significantly reduced menadione-stimulated phosphorylation of p38 and the p38 specific upstream kinase, MKK3/6 (Fig. 7, *A*, *F*, and *G*).

Activation of p38 MAP kinase signaling (42), as well as loss of BAD inhibition when Ser[136] is not phosphorylated (40, 41), have been implicated in cell death. As such, we aimed to determine the effects of menadione-induced oxidative stress on chondrocyte cell viability. Cell viability was reduced in a time-dependent manner to 27.9 $\pm$ 3.7% of control values after 9 h of menadione treatment (Fig. 7H). Pretreatment with the p38 specific inhibitor SB203580 or expression of MCAT abolished menadione-induced cell death (Fig. 7H).
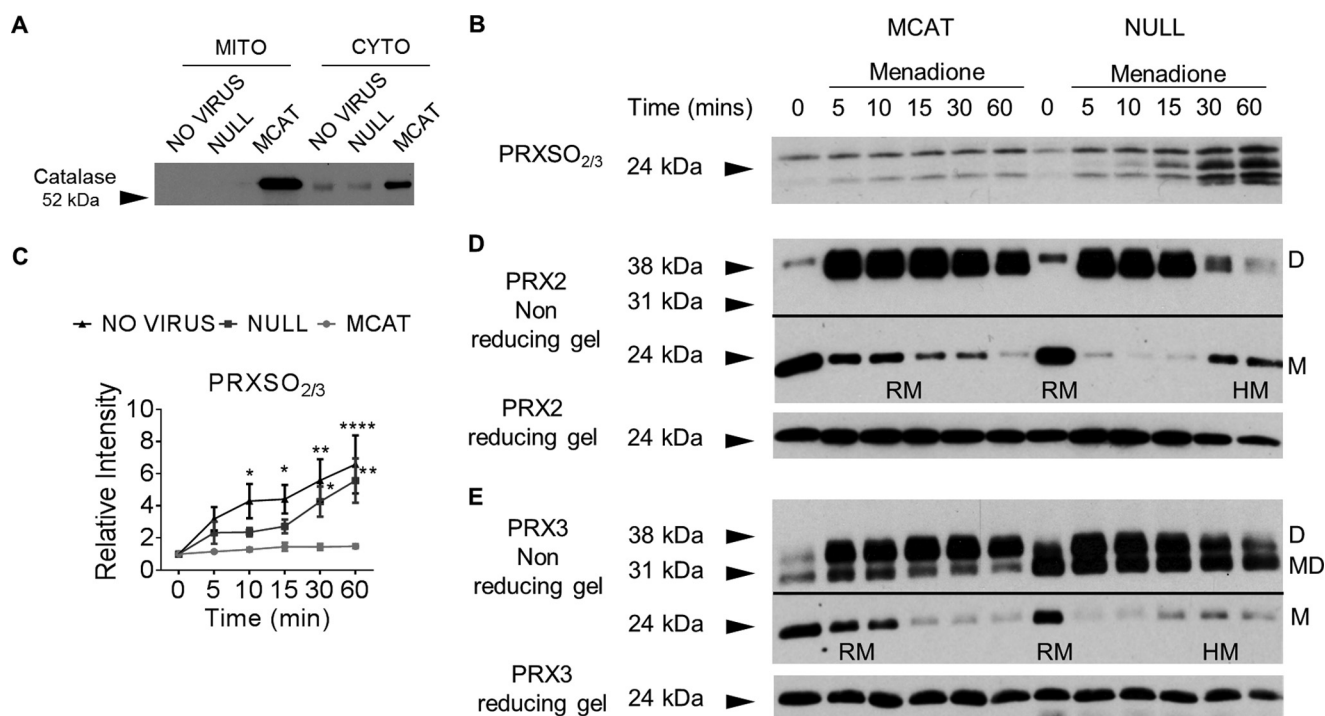
FIGURE 4. **Targeted expression of human catalase to the mitochondria attenuates menadione-induced PRX oxidation in human chondrocytes.** Confluent human articular chondrocytes were transduced with an adenovirus expressing mitochondrial catalase (MCAT), a null (empty) vector control, or no virus for 48 h prior to overnight incubation in serum-free medium and addition of 25 μM menadione for the indicated times to induce oxidative stress. Chondrocyte monolayers were incubated in 100 mM NEM for 10 min to alkylate reduced thiols prior to lysis, and cell lysates were prepared in NEM containing lysis buffer prior to immunoblotting. *A*, immunoblot of chondrocyte mitochondrial and cytosolic fractions showing expression of human catalase protein expression in unstimulated chondrocytes transduced with MCAT adenovirus, a null empty vector, or no virus. *B*, chondrocyte cell lysates transduced with MCAT adenovirus, a null empty vector, or no virus and then treated with menadione for the indicated times. Hyperoxidized PRXs were identified using the antibody to PRXSO$_{2/3}$. *C*, results of densitometric analysis from PRXSO$_{2/3}$ immunoblots from $n = 3$ independent donors. *D*, under nonreducing conditions, immunoblots for total PRX2 allowed for identification of the PRX2 reduced monomer (labeled *RM* on blots) and the hyperoxidized monomer (labeled *HM* on blots). PRX2 presented with an oxidized dimer (labeled *D* on blots). *E*, under nonreducing conditions, immunoblots for total PRX3 allowed for identification of the PRX3 reduced monomer (labeled *RM* on blots) and the hyperoxidized monomer (labeled *HM* on blots). PRX3 presented with an oxidized dimer (labeled *D* on blots), as well as a lower mixed disulfide band (labeled *MD* on blots). *Solid lines* on blots are used to separate different exposures from the same immunoblot. All immunoblots are representative results of $n = 3$ donors. The data are means $\pm$ S.E. normalized to untreated controls. *Asterisks* represent significant differences compared with control. *, $p < 0.05$; **, $p < 0.01$; ****, $p < 0.0001$ (ANOVA).
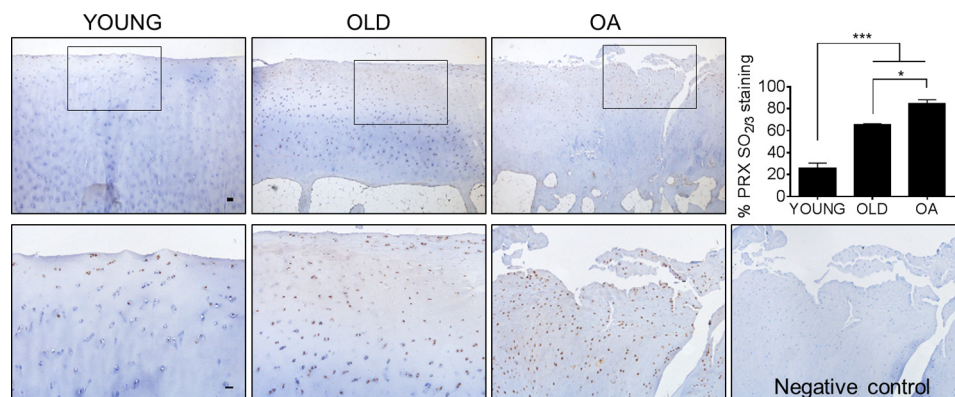

FIGURE 5. **Hyperoxidized PRX is observed in human cartilage from older adults and in osteoarthritic cartilage.** The levels of PRXSO$_{2/3}$ in normal younger, normal older, and osteoarthritic human knee cartilage was evaluated by immunohistochemistry using the antibody to PRXSO$_{2/3}$. Tissue sections were counterstained with hematoxylin. Human cartilage sections ($n = 4$ independent samples per group) were macroscopically graded as described under "Experimental Procedures." For these experiments, younger donors were <50 years old (mean age, 41.3 $\pm$ 6.1 years), and older donors were $\geq$50 years old (mean age, 73.3 $\pm$ 4.3 years). The average age of the OA patients was 79.3 $\pm$ 13.6 years. *Scale bar*, 100 μm. Representative negative control consists of primary incubation in antibody diluent without addition of anti-PRXSO$_{2/3}$. The data are presented as means $\pm$ S.E. of percentage PRXSO$_{2/3}$ stained cells for each condition. *Asterisks* represent significant differences compared with control. *, $p < 0.05$; ***, $p < 0.001$ (ANOVA).

Menadione-induced PRX Hyperoxidation and p38 Phosphorylation Are Attenuated in Cartilage from Mice Expressing Catalase Targeted to the Mitochondria—To investigate whether expression of mitochondrial catalase can modify cell signaling pathways in tissues, femoral cap cartilage explants were isolated from the hips of transgenic mice that express human catalase targeted to the mitochondria (MCAT mice) and from wild-type littermate controls (Fig. 8*A*). Corroborating our adenoviral expression data using isolated human chondrocytes, PRX hyperoxidation was lower in cartilage from MCAT mice compared with wild-type controls after menadione treatment (Fig. 8*B*). Menadione inhibition of IGF-1-mediated Akt phosphory-
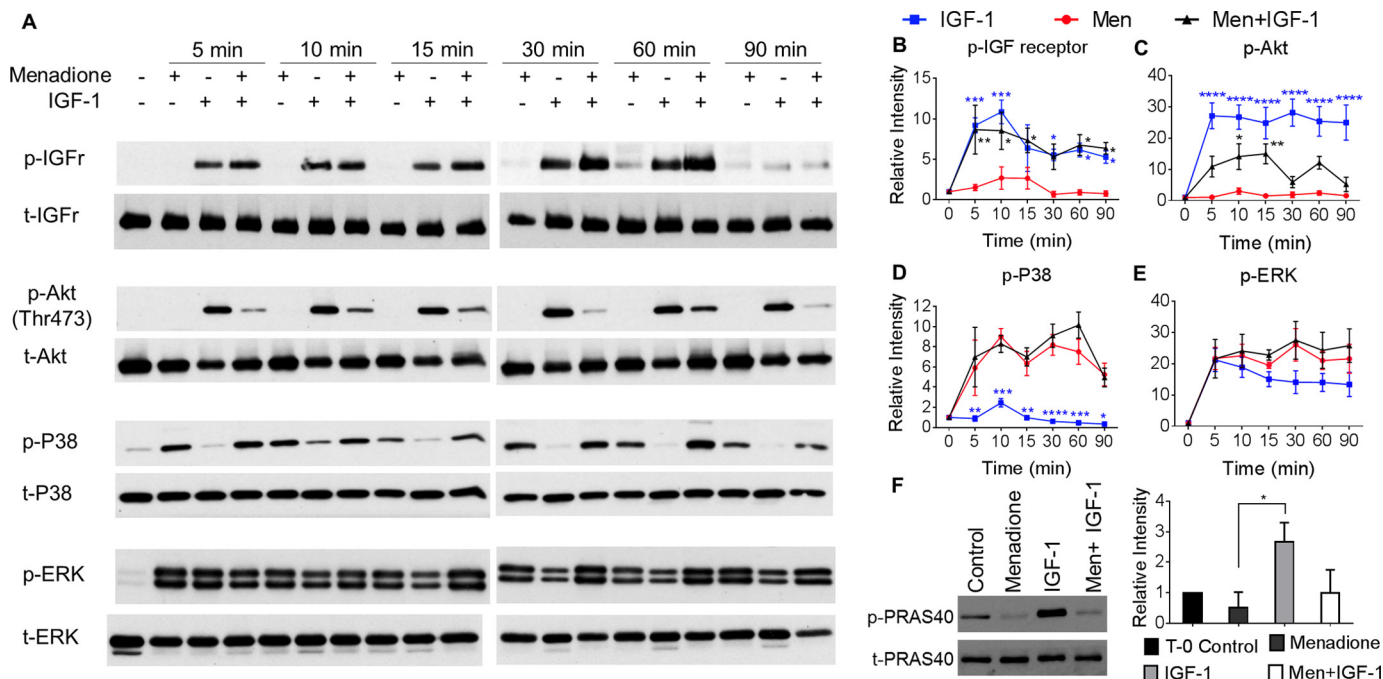
FIGURE 6. **Effect of oxidative stress on IGF-1 and MAP kinase signaling in normal human chondrocytes.** Confluent human articular chondrocytes cultured in serum-free medium were treated for the indicated times (0–90 min) with menadione (25 μM) or IGF-1 (50 ng/ml). For combined treatments, chondrocytes were pretreated with menadione (25 μM) for 30 min prior to IGF-1 treatment for the indicated times (0–90 min). After experimental incubations, cell lysates were prepared and immunoblotted under reducing conditions with antibodies to phosphorylated IGF receptor, Akt, ERK, and p38. The blots were then stripped and reprobed with respective total antibodies for loading controls. *A*, representative immunoblots from three independent experiments. *B–E*, results of densitometric analysis showing phosphorylation of IGF receptor, Akt, ERK, and p38. *F*, chondrocytes were treated for 30 min with 25 μM menadione, treated 30 min with 50 ng/ml IGF-1, or pretreated with menadione (30 min) prior to IGF-1 treatment (30 min), and immunoblotting was performed on reducing gels to probe for phosphorylation of PRAS40, a downstream marker of Akt activity. Phosphorylation of proteins was normalized to total protein as a loading control and presented as relative change compared with untreated controls. The data are presented as means ± S.E. from *n* = 3 donors. *Asterisks* represent significant differences compared with menadione treatment at that time point. *, $p < 0.05$; **, $p < 0.01$; ***, $p < 0.001$; ****, $p < 0.0001$ (ANOVA). *MEN*, menadione.

lation observed in wild-type mouse cartilage was abolished in cartilage from MCAT transgenic mice, demonstrating an enhanced ability of MCAT mice to activate pro-survival signaling proteins despite an oxidative challenge (Fig. 8, *C–E*). Furthermore, menadione-induced phosphorylation of p38 (but not ERK) observed in cartilage from wild-type mice was significantly reduced in cartilage from MCAT mice, suggesting that these transgenic mice are less susceptible to oxidative stress-induced pro-catabolic signaling (Fig. 8, *C*, *F*, and *G*).

MCAT Mice Develop Less Severe Age-related OA—Previous studies have demonstrated increased longevity and a reduction in age-related pathology in mice expressing catalase targeted to the mitochondria, in part because of decreased H$_2$O$_2$ production, attenuation of oxidative stress-induced damage, and maintenance of mitochondrial homeostasis (43, 44). To investigate whether MCAT mice are protected from age-associated OA, we assessed knee joints that had been previously collected from 18–33-month-old male MCAT and wild-type mice. Although not completely protected from age-related OA, MCAT mice were found to have less severe cartilage destruction compared with age-matched wild-type controls (Fig. 9), supporting a role for oxidative stress in age-related OA.

Discussion

Age-related oxidative stress has been proposed to contribute to the aging phenotype through the disruption of physiologic cell signaling pathways (3–5). The present findings in primary human chondrocytes isolated from younger and older adult

tissue donors support this hypothesis and implicate excessive oxidation of the PRXs as a potential mechanism by which oxidative stress disrupts signaling. PRX hyperoxidation, which inhibits peroxidase function and leads to increased levels of intracellular ROS, was significantly higher in chondrocytes isolated from older adults. In addition, the older adult cells demonstrated greater PRX hyperoxidation when challenged with menadione to induce oxidative stress, indicative of a lower level of anti-oxidant capacity compared with chondrocytes from younger adults. PRX hyperoxidation was associated with inhibition of pro-survival IGF-1-Akt signaling and up-regulation of pro-death signaling pathways. Reduction of ROS levels through targeted expression of mitochondrial catalase prevented PRX hyperoxidation. This was linked to increased Akt sensitivity and partial inhibition of the MKK-3/6-p38 pathway, which was associated with cell survival, as well as with a reduction in the severity of OA in aged mice.

Aging is a primary risk factor for OA, which is the most common cause of chronic disability in older adults and correlates with age-related redox imbalance and mitochondrial dysfunction (20–24). Although there are many potential mechanisms by which aging contributes to the development of OA, a common finding is an imbalance in anabolic and catabolic activity in the affected cartilage that promotes matrix destruction and is accompanied by increased chondrocyte death (45). IGF-1 is an important regulator of cartilage matrix synthesis and chondrocyte survival through the activity of PI-3 kinase-Akt pathway,
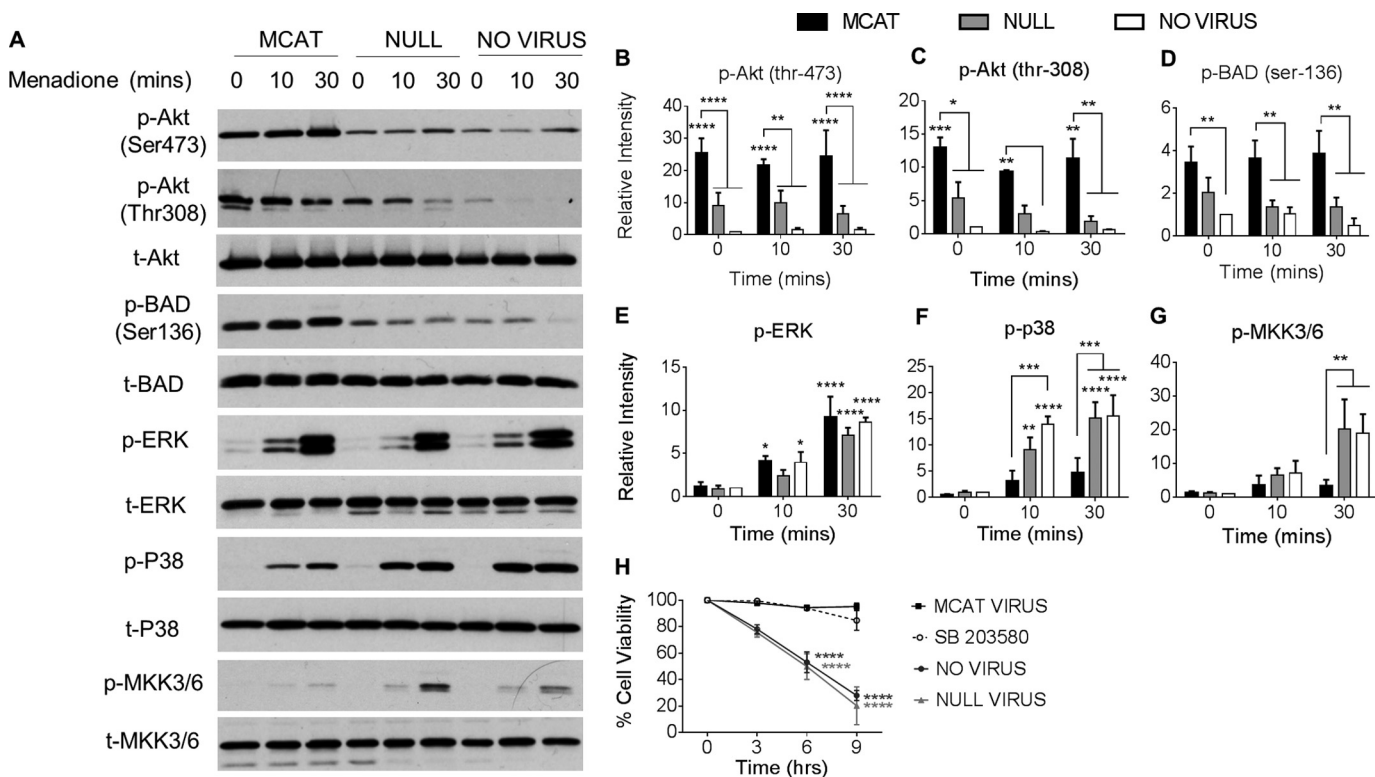
FIGURE 7. **Expression of mitochondrial-targeted catalase increases Akt phosphorylation and attenuates pro-apoptotic signaling induced by oxidative stress.** Confluent human articular chondrocytes were transduced with an adenovirus expressing mitochondrial catalase (MCAT), a null (empty) vector control, or no virus for 48 h prior to overnight incubation in serum-free medium and addition of 25 μM menadione for the indicated times (0–30 min) to induce oxidative stress. After experimental incubations, cell lysates were prepared and immunoblotted under reducing conditions with antibodies to phosphorylated Akt, BAD, ERK, p38, and MKK3/6. The blots were then stripped and reprobed with respective total antibodies for loading controls. *A*, representative immunoblots from three independent experiments. *B–G*, results of densitometric analysis showing phosphorylation of Akt, BAD, ERK, p38, and MKK3/6. Phosphorylation of proteins were normalized to total protein as a loading control and presented as fold change compared with untreated controls. The data are presented as means ± S.E. from $n = 3$ independent donors. *H*, chondrocytes treated with virus as above were treated with 25 μM menadione for the indicated times (0–9 h) to induce oxidative stress. For p38 inhibitor experiments, chondrocytes were treated with the p38 inhibitor SB203580 (10 μM) for 30 min prior to menadione treatment. Cell survival was assessed as described under "Experimental Procedures." The data are quantified as percentages of cell death (means ± S.E.) compared with control values from a minimum of three independent experiments. *Asterisks* represent significant differences compared with no virus untreated controls. *, $p < 0.05$; **, $p < 0.01$; ***, $p < 0.001$; ****, $p < 0.0001$ (ANOVA).

and therefore disrupted IGF-1 signaling, as the result of oxidative stress and PRX hyperoxidation, would be expected to promote the development of OA.

Although various forms of ROS, including superoxide, hydroxyl radical, and reactive nitrogen species, such as peroxynitrite, have been implicated as mediators of oxidative damage, the less reactive H_2O_2 has emerged as a key mediator of redox signaling (9, 10). H_2O_2 regulates specific signaling events through oxidatively modifying reactive cysteine thiols on redox-sensitive proteins (5, 6, 9, 10). These transient posttranslational modifications include oxidation to form sulfenic acid (Cys-SOH), which can be reduced back to the sulfhydryl state (Cys-SH) by active reductases that include the PRXs. Through reversible oxidation of specific cysteine residues, H_2O_2 has been shown to exert intracellular signaling capabilities, modifying a wide range of proteins including kinases, phosphatases, and transcription factors (46). However, despite participating in intracellular redox signaling, excessive production of H_2O_2 can induce oxidative damage to DNA, lipids, and proteins, and therefore controlled and efficient removal of high levels of H_2O_2 is required.

The highly abundant typical 2-Cys PRXs were chosen as a focus of this study because they catalyze the specific reduction

of H_2O_2 through a conserved catalytic cysteine residue that serves as a site of H_2O_2-dependent oxidation, thereby conferring efficient cellular antioxidant activity through H_2O_2 detoxification (11). We used complementary immunoblotting techniques with antibodies to PRXSO$_{2/3}$, as well as evaluation of oxidized PRX2 and PRX3 on nonreducing gels to evaluate PRX oxidation in chondrocytes. In accordance with findings from Cox *et al.* (33), we found that addition of NEM to cultured cells just prior to lysis prevented the formation of oxidized dimers of PRX2 and PRX3 in untreated control cells that was seen when IAM was used to alkylate thiols during lysis. However, menadione treatment was found to increase the levels of hyperoxidized PRX2 and PRX3 detected with either method indicating that ROS generated by menadione rather than cell lysis was responsible for PRX hyperoxidation.

Recent evidence shows that PRXs participate in direct regulation of intracellular signal transduction pathways (13, 47). The catalytic activity of some eukaryotic PRXs is highly sensitive to reversible inhibition by H_2O_2-mediated hyperoxidation, and oxidative inactivation of PRXs is considered as a key transient mechanism to allow local H_2O_2 levels to accumulate and initiate redox-signaling events (11). Additionally, PRXs can directly regulate H_2O_2 signal transduction through thiol-disul-
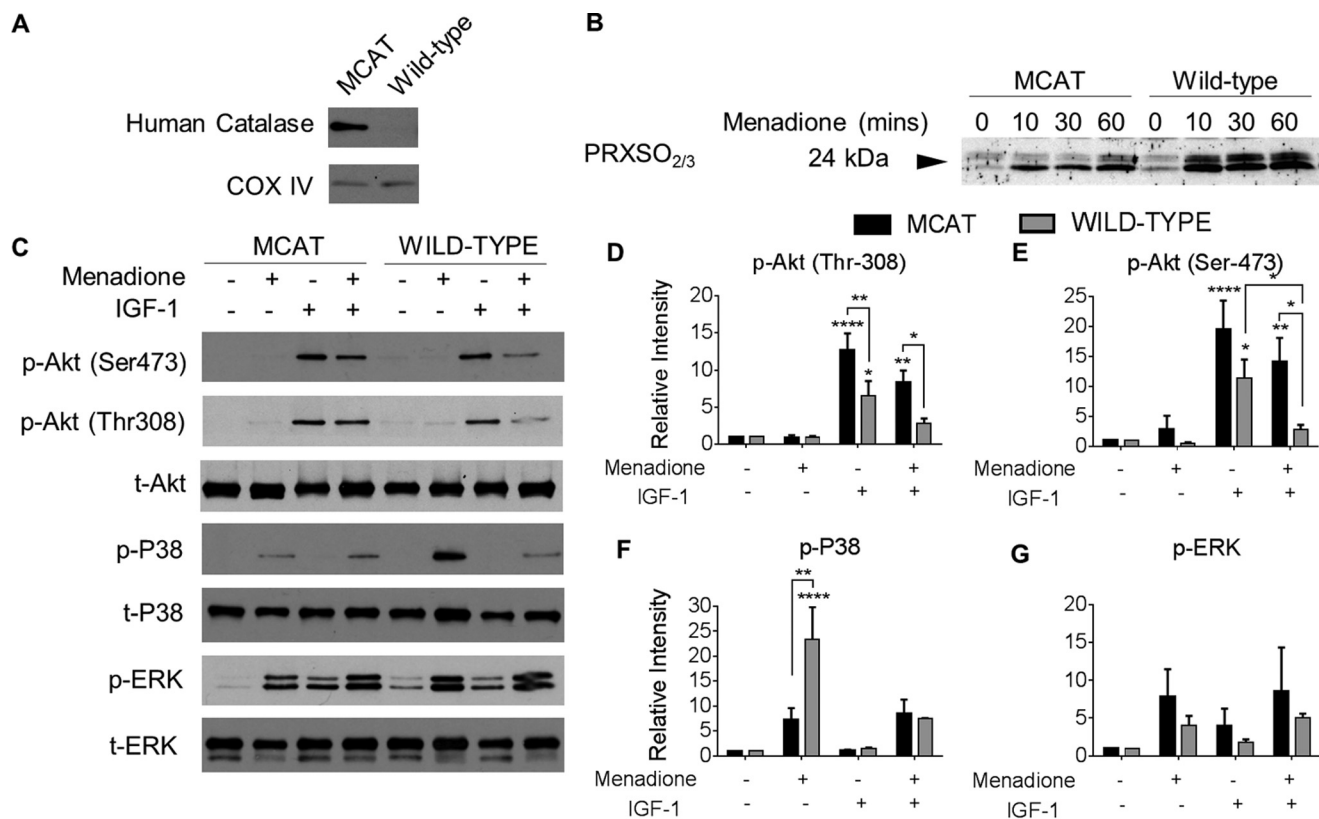
FIGURE 8. **Effect of oxidative stress on PRX hyperoxidation and kinase phosphorylation in chondrocytes from MCAT and wild-type mice.** Femoral head cartilage explants from the hip joints of 4-week-old MCAT and wild-type mice were isolated and cultured in serum-supplemented medium for 48 h prior to overnight incubation in serum-free medium. Femoral head cartilage explants were treated with menadione (25 μM), IGF-1 (50 ng/ml), or combined treatments as indicated. Cell lysates were prepared by homogenization of explants as described under "Experimental Procedures." *A*, cell lysates were immunoblotted for human catalase and for COX IV as a mitochondrial protein loading control. *B*, femoral cap cartilage explants from MCAT and wild-type mice were cultured in menadione for 0–60 min prior to incubation in NEM (100 mM, 10 min) to alkylate reduced thiols prior to lysis. Femoral caps were disrupted and homogenized in lysis buffer containing NEM. Hyperoxidized PRXs were detected by immunoblot using the PRX-SO$_{2/3}$ antibody. *C*, for analysis of signaling, femoral cap cartilage explants were treated with menadione (30 min), IGF-1 (30 min), or pretreated with menadione (30 min) prior to IGF-1 treatment (30 min). Representative blots from $n = 3$ independent experiments are shown. *D–G*, results of densitometric analysis showing phosphorylation of Akt, p38, and ERK. Phosphorylation of proteins were normalized to total protein as a loading control and presented as fold change from untreated control. All data are presented as means $\pm$ S.E. from $n = 3$ independent experiments. *Asterisks* represent significant differences compared with control. *, $p < 0.05$; **, $p < 0.01$; ***, $p < 0.001$; ****, $p < 0.0001$ (ANOVA).
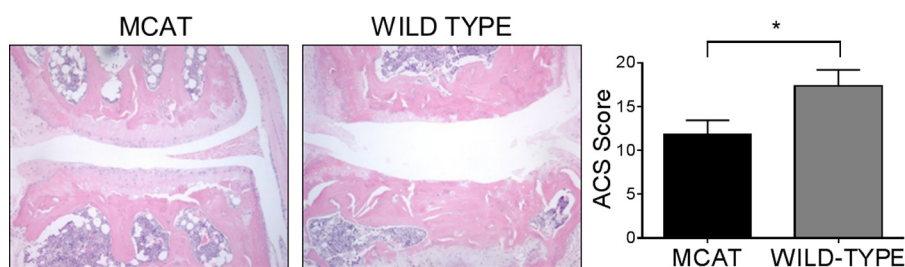

FIGURE 9. **MCAT mice develop less severe age-related OA.** Histological evaluation of knee joints from MCAT and wild-type mice aged 18–33 months. Sections from age-matched wild-type and MCAT mice are shown. Independent blinded histological assessment of OA severity was conducted on the medial and lateral tibial plateaus using an OA grading scheme (Articular Cartilage Structure score). The data are presented as means $\pm$ S.E. of the medial plus lateral tibial plateau Articular Cartilage Structure Scores $n = 5$ wild-type and $n = 6$ MCAT mice. The *asterisk* represents a significant difference between mouse phenotypes. *, $p < 0.05$ (ANOVA).

fide exchange, allowing the oxidative signal to be transferred to other redox sensitive proteins with a lower affinity for H_2O_2 than PRXs (13, 47).

PRXs have recently been shown to participate in signal transduction pathways that regulate resistance to oxidative stress and lifespan extension through regulation of JNK/FOXO signaling in *Drosophila melanogaster* (48). We did not observe an increase in chondrocyte JNK phosphorylation in response to menadione-induced oxidative stress but rather found increased

phosphorylation of MMK-3/6 and p38 along with inhibition of IGF-1-mediated Akt activation. This was consistent with previous studies demonstrating that PRX and thioredoxin can act as negative regulators of cell death pathways by direct inhibition of the ASK1-MKK3/6-p38 pathway in mice (49) and cell lines (50), an effect inhibited by oxidative stress. ROS-induced inhibition of Akt was also found to result in activation of the ASK1-MKK3/6-p38 pathway, which caused cell death in several cell lines (51).

Whether the PI3K-Akt pathway is activated or inhibited by ROS depends on the redox status of the cell. Previous studies have shown that low levels of ROS promote IGF-1-PI-3 kinase-Akt signaling through reversible oxidative inhibition of upstream phosphatases including PTEN (phosphatase and tensin homolog) and PTP1B (protein-tyrosine phosphatase 1B) (52). This occurs through oxidation at specific cysteine residues in the phosphatase catalytic site resulting in inhibition of phosphatase activity leading to enhancement of IGF signaling. Conversely, recent evidence demonstrates that high levels of mitochondrial superoxide promote PTEN- and PTP1B-mediated dephosphorylation of the IGF-1 receptor, which attenuates IGF signaling (53). Our data demonstrate that in the presence of high levels of ROS generated by menadione, inhibition of IGF-1-mediated Akt phosphorylation occurs despite no change in IGF-1 receptor phosphorylation. In a previous study (32), we found that oxidative stress conditions in chondrocytes stimulated phosphorylation of IRS-1 on inhibitory serine residues and inhibited phosphorylation of the activating tyrosine residues, which would be one mechanism for the downstream loss of Akt phosphorylation.

In the present study, expression of mitochondrial catalase restored phospho-Akt levels; promoted phosphorylation of the downstream target protein BAD at Ser^{136}, which inhibits pro-apoptotic BAD activity; and reduced MKK3/6-p38 activation. MCAT expression restored cell viability and, alongside the observation that pharmacological inhibition of p38 completely abolished cell death, demonstrates the effect of oxidative stress to alter physiological signaling pathways in human chondrocytes that ultimately regulate cell survival.

The close interplay between H_2O_2 production and PRX hyperoxidation needs to be tightly regulated to avoid oxidative stress and aberrant redox signaling. Genetic deletion of PRX levels alters redox balance and accelerates aging in yeast, flies, worms, and mice (17), but the mechanisms by which PRX levels are altered with age in primary cells, and the effects on cell signaling have not been defined. Our studies using primary human chondrocytes isolated from young and older adult tissue donors did not reveal a decline in the overall levels of PRX2 or PRX3 with age. Instead, we found that older chondrocytes displayed an increased level of basal PRX hyperoxidation compared with younger chondrocytes and displayed an increased sensitivity toward hyperoxidation when exposed to oxidative stress. These findings were corroborated by immunohistochemical data, which showed significantly elevated PRXSO$_{2/3}$ immunopositivity in cartilage tissue sections from older donors, which indicates a diminished PRX reducing capacity in these aging tissues. The increased susceptibility of PRXs to hyperoxidation in older chondrocytes suggests an age-related loss of reducing capacity. We have not found differences in the levels of proteins involved in PRX reduction (sulfiredoxin, thioredoxin 1, or thioredoxin reductase 2) in young and old chondrocytes (data not shown). However, in previous work we identified an age-related increase in oxidized glutathione, as well as an increase in the ratio of oxidized relative to reduced GSH levels, in human articular chondrocytes, which is implicit with an age-related decrease in reducing capacity (21). In agreement, the work of others demonstrates increased PRX hyperoxidation

in aged mice and yeast, as well as an age-associated decrease in the ability of sulfiredoxin to reduce hyperoxidized PRXs (17). Increased PRX hyperoxidation in our study was also evident in OA cartilage, supporting the hypothesis that oxidative stress-mediated PRX hyperoxidation and subsequent redox imbalance may be a common phenotype in aging tissues and may contribute to age-related disease.

The mitochondrion is an important source of ROS, and production of excessive amounts caused by mitochondrial dysfunction has been implicated in age-related conditions including OA (1, 4, 8). The conditional deletion of mitochondrial superoxide dismutase in chondrocytes was reported to result in premature age-related OA in mice (54). These findings and our result of less severe OA in the MCAT mice are consistent with mitochondrial redox imbalance as a mechanism contributing to OA. Expression of catalase targeted to the mitochondria counteracted menadione-induced PRX hyperoxidation, abolished cell death in human chondrocytes, and restored IGF-1-mediated Akt signaling in cultured human cells and cartilage explants from MCAT mice. These findings, combined with the observation that the mitochondrial PRX isoform, PRX3, was hyperoxidized more rapidly than the cytosolic isoform PRX2, suggests that the mitochondria were an important source of ROS in our oxidative stress experiments.

However, we also observed oxidation of the cytosolic PRX2 and altered phosphorylation of proteins in signaling pathways that are predominantly cytosolic, indicating that cytosolic oxidative stress was also induced by menadione. Indeed, menadione has been shown to increase levels of ROS in multiple subcellular compartments (30), deplete reduced glutathione (55, 56), decrease NADPH levels (57), and inhibit metabolic enzyme activity (58), all of which may alter downstream signaling events. It is also important to note that MCAT expression did not completely inhibit menadione-induced PRX oxidation but primarily hyperoxidation. This could have been due to effects of menadione that were separate from H_2O_2 generation or to the rapid kinetics by which H_2O_2 reacts with PRXs. Because we noted a rapid increase in levels of H_2O_2 in cells treated with menadione, it is unlikely that MCAT overexpression would be sufficient to outcompete PRXs for all of the H_2O_2 generated.

Collectively, this study implicates oxidative stress and associated PRX hyperoxidation as a key mechanism contributing to an age-associated disruption in signal transduction that can result in chondrocyte death and promote the development of OA. Further work is needed to determine whether PRX hyperoxidation plays a causal role in this process and to define the mechanisms responsible. Given the critical role of PRXs in controlling the level of intracellular H_2O_2, inhibition of PRX function by hyperoxidation would be expected to result in excessive levels of H_2O_2, resulting in oxidation of signaling proteins normally protected by the PRXs. Targeting mitochondrial overproduction of ROS has been considered as a therapeutic approach for age-related conditions such as cardiovascular disease (59). The present findings suggest that this approach may be of benefit for OA as well. Alternatively, restoring redox balance and normal physiological signaling through the modulation of PRX oxidation may represent a novel therapeutic

approach for the treatment of age-related cellular dysfunction and disease.

Author Contributions—This study was conceived by R. F. L. and J. A. C. The data were acquired by J. A. C., S. T. W., M. A. R., C. S. C., and S. C. and were analyzed and interpreted by all authors. S. C. provided human tissue. The manuscript was drafted by J. A. C. and R. F. L., and all authors contributed to revising the manuscript for scientific content. The final version was approved by all authors.

References

1. López-Otín, C., Blasco, M. A., Partridge, L., Serrano, M., and Kroemer, G. (2013) The hallmarks of aging. *Cell* **153,** 1194–1217
2. van Deursen, J. M. (2014) The role of senescent cells in ageing. *Nature* **509,** 439–446
3. Balaban, R. S., Nemoto, S., and Finkel, T. (2005) Mitochondria, oxidants, and aging. *Cell* **120,** 483–495
4. Chan, D. C. (2006) Mitochondria: dynamic organelles in disease, aging, and development. *Cell* **125,** 1241–1252
5. Finkel, T. (2011) Signal transduction by reactive oxygen species. *J. Cell Biol.* **194,** 7–15
6. Jones, D. P. (2006) Extracellular redox state: refining the definition of oxidative stress in aging. *Rejuvenation Res.* **9,** 169–181
7. Veal, E. A., Day, A. M., and Morgan, B. A. (2007) Hydrogen peroxide sensing and signaling. *Mol. Cell* **26,** 1–14
8. Bratic, A., and Larsson, N. G. (2013) The role of mitochondria in aging. *J. Clin. Invest.* **123,** 951–957
9. Cross, J. V., and Templeton, D. J. (2006) Regulation of signal transduction through protein cysteine oxidation. *Antioxid. Redox Signal.* **8,** 1819–1827
10. Klomsiri, C., Karplus, P. A., and Poole, L. B. (2011) Cysteine-based redox switches in enzymes. *Antioxid. Redox Signal.* **14,** 1065–1077
11. Wood, Z. A., Poole, L. B., and Karplus, P. A. (2003) Peroxiredoxin evolution and the regulation of hydrogen peroxide signaling. *Science* **300,** 650–653
12. Randall, L. M., Ferrer-Sueta, G., and Denicola, A. (2013) Peroxiredoxins as preferential targets in H_2O_2-induced signaling. *Methods Enzymol.* **527,** 41–63
13. Sobotta, M. C., Liou, W., Stöcker, S., Talwar, D., Oehler, M., Ruppert, T., Scharf, A. N., and Dick, T. P. (2015) Peroxiredoxin-2 and STAT3 form a redox relay for H_2O_2 signaling. *Nat. Chem. Biol.* **11,** 64–70
14. Delaunay, A., Pflieger, D., Barrault, M. B., Vinh, J., and Toledano, M. B. (2002) A thiol peroxidase is an H_2O_2 receptor and redox-transducer in gene activation. *Cell* **111,** 471–481
15. Peskin, A. V., Dickerhof, N., Poynton, R. A., Paton, L. N., Pace, P. E., Hampton, M. B., and Winterbourn, C. C. (2013) Hyperoxidation of peroxiredoxins 2 and 3: rate constants for the reactions of the sulfenic acid of the peroxidatic cysteine. *J. Biol. Chem.* **288,** 14170–14177
16. Lowther, W. T., and Haynes, A. C. (2011) Reduction of cysteine sulfinic acid in eukaryotic, typical 2-Cys peroxiredoxins by sulfiredoxin. *Antioxid. Redox Signal.* **15,** 99–109
17. Nyström, T., Yang, J., and Molin, M. (2012) Peroxiredoxins, gerontogenes linking aging to genome instability and cancer. *Genes Dev.* **26,** 2001–2008
18. Loeser, R. F., Goldring, S. R., Scanzello, C. R., and Goldring, M. B. (2012) Osteoarthritis: a disease of the joint as an organ. *Arthritis Rheum.* **64,** 1697–1707
19. Loeser, R. F. (2013) Aging processes and the development of osteoarthritis. *Curr. Opin. Rheumatol.* **25,** 108–113
20. Loeser, R. F., Carlson, C. S., Del Carlo, M., and Cole, A. (2002) Detection of nitrotyrosine in aging and osteoarthritic cartilage: correlation of oxidative damage with the presence of interleukin-1β and with chondrocyte resistance to insulin-like growth factor 1. *Arthritis Rheum.* **46,** 2349–2357
21. Carlo, M. D., Jr., and Loeser, R. F. (2003) Increased oxidative stress with aging reduces chondrocyte survival: correlation with intracellular glutathione levels. *Arthritis Rheum.* **48,** 3419–3430
22. Gavriilidis, C., Miwa, S., von Zglinicki, T., Taylor, R. W., and Young, D. A. (2013) Mitochondrial dysfunction in osteoarthritis is associated with down-regulation of superoxide dismutase 2. *Arthritis Rheum.* **65,** 378–387
23. Blanco, F. J., Rego, I., and Ruiz-Romero, C. (2011) The role of mitochondria in osteoarthritis. *Nat. Rev. Rheumatol.* **7,** 161–169
24. Ruiz-Romero, C., Calamia, V., Mateos, J., Carreira, V., Martínez-Gomariz, M., Fernández, M., and Blanco, F. J. (2009) Mitochondrial dysregulation of osteoarthritic human articular chondrocytes analyzed by proteomics: a decrease in mitochondrial superoxide dismutase points to a redox imbalance. *Mol. Cell. Proteomics* **8,** 172–189
25. Loeser, R. F., Pacione, C. A., and Chubinskaya, S. (2003) The combination of insulin-like growth factor 1 and osteogenic protein 1 promotes increased survival of and matrix synthesis by normal and osteoarthritic human articular chondrocytes. *Arthritis Rheum.* **48,** 2188–2196
26. Yin, W., Park, J. I., and Loeser, R. F. (2009) Oxidative stress inhibits insulin-like growth factor-I induction of chondrocyte proteoglycan synthesis through differential regulation of phosphatidylinositol 3-kinase-Akt and MEK-ERK MAPK signaling pathways. *J. Biol. Chem.* **284,** 31972–31981
27. Loeser, R. F., Gandhi, U., Long, D. L., Yin, W., and Chubinskaya, S. (2014) Aging and oxidative stress reduce the response of human articular chondrocytes to insulin-like growth factor 1 and osteogenic protein 1. *Arthritis Rheumatol.* **66,** 2201–2209
28. Schriner, S. E., Linford, N. J., Martin, G. M., Treuting, P., Ogburn, C. E., Emond, M., Coskun, P. E., Ladiges, W., Wolf, N., Van Remmen, H., Wallace, D. C., and Rabinovitch, P. S. (2005) Extension of murine life span by overexpression of catalase targeted to mitochondria. *Science* **308,** 1909–1911
29. Criddle, D. N., Gillies, S., Baumgartner-Wilson, H. K., Jaffar, M., Chinje, E. C., Passmore, S., Chvanov, M., Barrow, S., Gerasimenko, O. V., Tepikin, A. V., Sutton, R., and Petersen, O. H. (2006) Menadione-induced reactive oxygen species generation via redox cycling promotes apoptosis of murine pancreatic acinar cells. *J. Biol. Chem.* **281,** 40485–40492
30. Loor, G., Kondapalli, J., Schriewer, J. M., Chandel, N. S., Vanden Hoek, T. L., and Schumacker, P. T. (2010) Menadione triggers cell death through ROS-dependent mechanisms involving PARP activation without requiring apoptosis. *Free Radic. Biol. Med.* **49,** 1925–1936
31. Schneider, C. A., Rasband, W. S., and Eliceiri, K. W. (2012) NIH Image to ImageJ: 25 years of image analysis. *Nat. Methods* **9,** 671–675
32. Vilela, M., Halidi, N., Besson, S., et al. (2013) Fluctuation analysis of activity biosensor images for the study of information flow in signaling pathways. In *Fluorescence Fluctuation Spectroscopy* (Tetin, S. Y., ed) Vol. 519, pp. 253–276, Elsevier Academic Press Inc., San Diego, CA
33. Cox, A. G., Winterbourn, C. C., and Hampton, M. B. (2010) Measuring the redox state of cellular peroxiredoxins by immunoblotting. *Methods Enzymol.* **474,** 51–66
34. Del Carlo, M., Jr., and Loeser, R. F. (2002) Nitric oxide-mediated chondrocyte cell death requires the generation of additional reactive oxygen species. *Arthritis Rheum.* **46,** 394–403
35. Levy, Y. D., Hasegawa, A., Patil, S., Koziol, J. A., Lotz, M. K., and D'Lima, D. D. (2013) Histopathological changes in the human posterior cruciate ligament during aging and osteoarthritis: correlations with anterior cruciate ligament and cartilage changes. *Ann. Rheum. Dis.* **72,** 271–277
36. Ulici, V., James, C. G., Hoenselaar, K. D., and Beier, F. (2010) Regulation of gene expression by PI3K in mouse growth plate chondrocytes. *PLoS One* **5,** e8866
37. McNulty, M. A., Loeser, R. F., Davey, C., Callahan, M. F., Ferguson, C. M., and Carlson, C. S. (2011) A comprehensive histological assessment of

osteoarthritis lesions in mice. *Cartilage* **2,** 354–363

38. Gutscher, M., Sobotta, M. C., Wabnitz, G. H., Ballikaya, S., Meyer, A. J., Samstag, Y., and Dick, T. P. (2009) Proximity-based protein thiol oxidation by H_2O_2-scavenging peroxidases. *J. Biol. Chem.* **284,** 31532–31540

39. Vander Haar, E., Lee, S. I., Bandhakavi, S., Griffin, T. J., and Kim, D. H. (2007) Insulin signalling to mTOR mediated by the Akt/PKB substrate PRAS40. *Nat. Cell Biol.* **9,** 316–323

40. Datta, S. R., Dudek, H., Tao, X., Masters, S., Fu, H., Gotoh, Y., and Greenberg, M. E. (1997) Akt phosphorylation of BAD couples survival signals to the cell-intrinsic death machinery. *Cell* **91,** 231–241

41. del Peso, L., González-García, M., Page, C., Herrera, R., and Nuñez, G. (1997) Interleukin-3-induced phosphorylation of BAD through the protein kinase Akt. *Science* **278,** 687–689

42. Pelletier, J. P., Fernandes, J. C., Jovanovic, D. V., Reboul, P., and Martel-Pelletier, J. (2001) Chondrocyte death in experimental osteoarthritis is mediated by MEK 1/2 and p38 pathways: role of cyclooxygenase-2 and inducible nitric oxide synthase. *J. Rheumatol.* **28,** 2509–2519

43. Dai, D. F., Santana, L. F., Vermulst, M., Tomazela, D. M., Emond, M. J., MacCoss, M. J., Gollahon, K., Martin, G. M., Loeb, L. A., Ladiges, W. C., and Rabinovitch, P. S. (2009) Overexpression of catalase targeted to mitochondria attenuates murine cardiac aging. *Circulation* **119,** 2789–2797

44. Lee, H. Y., Choi, C. S., Birkenfeld, A. L., Alves, T. C., Jornayvaz, F. R., Jurczak, M. J., Zhang, D., Woo, D. K., Shadel, G. S., Ladiges, W., Rabinovitch, P. S., Santos, J. H., Petersen, K. F., Samuel, V. T., and Shulman, G. I. (2010) Targeted expression of catalase to mitochondria prevents age-associated reductions in mitochondrial function and insulin resistance. *Cell Metab.* **12,** 668–674

45. Lotz, M., and Loeser, R. F. (2012) Effects of aging on articular cartilage homeostasis. *Bone* **51,** 241–248

46. Rhee, S. G., Chae, H. Z., and Kim, K. (2005) Peroxiredoxins: a historical overview and speculative preview of novel mechanisms and emerging concepts in cell signaling. *Free Radic. Biol. Med.* **38,** 1543–1552

47. Pace, P. E., Peskin, A. V., Han, M. H., Hampton, M. B., and Winterbourn, C. C. (2013) Hyperoxidized peroxiredoxin 2 interacts with the protein disulfide-isomerase ERp46. *Biochem. J.* **453,** 475–485

48. Lee, K. S., Iijima-Ando, K., Iijima, K., Lee, W. J., Lee, J. H., Yu, K., and Lee, D. S. (2009) JNK/FOXO-mediated neuronal expression of fly homologue of peroxiredoxin II reduces oxidative stress and extends life span. *J. Biol. Chem.* **284,** 29454–29461

49. Hsieh, C. C., and Papaconstantinou, J. (2006) Thioredoxin-ASK1 complex levels regulate ROS-mediated p38 MAPK pathway activity in livers of aged and long-lived Snell dwarf mice. *FASEB J.* **20,** 259–268

50. Kim, S. Y., Kim, T. J., and Lee, K. Y. (2008) A novel function of peroxiredoxin 1 (Prx-1) in apoptosis signal-regulating kinase 1 (ASK1)-mediated signaling pathway. *FEBS Lett.* **582,** 1913–1918

51. Ahn, J., Won, M., Choi, J. H., Kim, Y. S., Jung, C. R., Im, D. S., Kyun, M. L., Lee, K., Song, K. B., and Chung, K. S. (2013) Reactive oxygen species-mediated activation of the Akt/ASK1/p38 signaling cascade and p21(Cip1) downregulation are required for shikonin-induced apoptosis. *Apoptosis* **18,** 870–881

52. Loh, K., Deng, H., Fukushima, A., Cai, X., Boivin, B., Galic, S., Bruce, C., Shields, B. J., Skiba, B., Ooms, L. M., Stepto, N., Wu, B., Mitchell, C. A., Tonks, N. K., Watt, M. J., *et al.* (2009) Reactive oxygen species enhance insulin sensitivity. *Cell Metab.* **10,** 260–272

53. Singh, K., Maity, P., Krug, L., Meyer, P., Treiber, N., Lucas, T., Basu, A., Kochanek, S., Wlaschek, M., Geiger, H., and Scharffetter-Kochanek, K. (2015) Superoxide anion radicals induce IGF-1 resistance through concomitant activation of PTP1B and PTEN. *EMBO Mol Med* **7,** 59–77

54. Koike, M., Nojiri, H., Ozawa, Y., Watanabe, K., Muramatsu, Y., Kaneko, H., Morikawa, D., Kobayashi, K., Saita, Y., Sasho, T., Shirasawa, T., Yokote, K., Kaneko, K., and Shimizu, T. (2015) Mechanical overloading causes mitochondrial superoxide and SOD2 imbalance in chondrocytes resulting in cartilage degeneration. *Sci. Rep.* **5,** 11722

55. Di Monte, D., Ross, D., Bellomo, G., Eklöw, L., and Orrenius, S. (1984) Alterations in intracellular thiol homeostasis during the metabolism of menadione by isolated rat hepatocytes. *Arch. Biochem. Biophys.* **235,** 334–342

56. Toxopeus, C., van Holsteijn, I., Thuring, J. W., Blaauboer, B. J., and Noordhoek, J. (1993) Cytotoxicity of menadione and related quinones in freshly isolated rat hepatocytes: effects on thiol homeostasis and energy charge. *Arch. Toxicol.* **67,** 674–679

57. Smith, P. F., Alberts, D. W., and Rush, G. F. (1987) Menadione-induced oxidative stress in hepatocytes isolated from fed and fasted rats: the role of NADPH-regenerating pathways. *Toxicol. Appl. Pharmacol.* **89,** 190–201

58. McAmis, W. C., Schaeffer, R. C., Jr., Baynes, J. W., and Wolf, M. B. (2003) Menadione causes endothelial barrier failure by a direct effect on intracellular thiols, independent of reactive oxidant production. *Biochim. Biophys. Acta* **1641,** 43–53

59. Dai, D. F., Rabinovitch, P. S., and Ungvari, Z. (2012) Mitochondria and cardiovascular aging. *Circ. Res.* **110,** 1109–1124